ELSEVIER

Cancer Genetics and Cytogenetics 180 (2008) 100–109

Cancer Genetics and Cytogenetics

Lead article

The UOK 257 cell line: a novel model for studies of the human Birt–Hogg–Dubé gene pathway

Youfeng Yang[a], Hesed M. Padilla-Nash[b], Manish A. Vira[a], Mones S. Abu-Asab[c], Daniel Val[c], Robert Worrell[a], Maria Tsokos[c], Maria J. Merino, Christian P. Pavlovich[a,1], Thomas Ried[b], W. Marston Linehan[a], Cathy D. Vocke[a,*]

[a]*Urologic Oncology Branch, Center for Cancer Research, National Cancer Institute, National Institutes of Health, Building 10, Room 1W-5888, Bethesda, MD 20892*

[b]*Genetics Branch, Center for Cancer Research, National Cancer Institute, National Institutes of Health, Bethesda, MD*

[c]*Laboratory of Pathology, Center for Cancer Research, National Cancer Institute, National Institutes of Health, Bethesda, MD*

Received 28 September 2007; accepted 16 October 2007

Abstract The establishment, characterization, and tumorigenicity of a new epithelial cell line (UOK 257) derived from human renal carcinoma of an individual with Birt–Hogg–Dubé (BHD) syndrome are reported. Unlike other established renal tumor cell lines from sporadic renal cell carcinoma, this is the first established renal tumor cell line of BHD, an inheritable neoplastic syndrome. The isolated tumor cells display loss of contact inhibition in vitro, and produce subcutaneous tumors in mouse xenografts. Histopathologic, ultrastructural, and cytogenetic characterizations of the established tumor cells are reported. Cytogenetic analysis using spectral karyotyping on UOK 257 cells revealed 17p loss and a near-triploid and aneuploid karyotype with multiple fluorescence in situ hybridization analysis using a locus-specific gene probe for *MYC*. The result demonstrates that the established tumor cells consist of two cell populations, one containing four and one containing five copies of the *MYC* oncogene. © 2008 Elsevier Inc. All rights reserved.

1. Introduction

Birt–Hogg–Dubé (BHD) is a rare, inherited autosomal dominant cancer syndrome caused by mutations in the *FLCN* gene (also known as *BHD*), which is located on the short arm of chromosome 17 (17p11.2) [1–3]. Patients affected with BHD are at risk to develop cutaneous fibrofolliculomas, pulmonary cysts, spontaneous pneumothorax, and bilateral renal tumors. As previously described, the renal tumors from BHD patients may display multiple histologic types, including chromophobe, oncocytoma, clear cell, papillary, and hybrid oncocytic. The hybrid oncocytic type is unique to BHD patients, with features of both chromophobe renal cell carcinoma (RCC) and oncocytoma [2,4,5]. Furthermore, a mixture of several distinct populations of tumor cells can be seen in hybrid tumors [6]. The presence of these distinct histologic types may reflect differences in germline and somatic mutations of the *FLCN* gene in the various BHD tumors [1,7,8].

Investigators have long recognized the potential value of a cell culture system as useful tool for studying hereditary human renal carcinomas, and the availability of human hereditary cancer cell cultures has led to a better understanding of the pathways affecting the growth and structure of those malignant cells [7,9]. From the current American Type Culture Collection (ATCC) online cell line indexes, 11 out of 950 described cancer cell lines have been derived from the human kidney (http://www.atcc.org/common/documents/pdf/CellCatalog/TumorLines.pdf). Currently, none of those are known to be derived directly from hereditary RCC [10,11].

Despite decades of effort, subsequent attempts to cultivate cells from hereditary renal carcinoma epithelial cells have been unsuccessful. Considering that the exact molecular and cellular events underlying the genesis of the BHD syndrome and the precise functions and pathways of the *FLCN* gene have yet to be established, there is a need for tumor cell lines established directly from BHD tumor

* Corresponding author. Tel.: (301) 402-1963; fax: (301) 402-0922.
E-mail address: vockec@mail.nih.gov (C.D. Vocke).
[1] Current address: Brady Urological Institute, Johns Hopkins Bayview Medical Center, Baltimore, MD.

0165-4608/08/$ – see front matter © 2008 Elsevier Inc. All rights reserved.
doi:10.1016/j.cancergencyto.2007.10.010

samples. These cell lines could then serve as valuable tools for the study of the molecular mechanism of genesis, particularly for the BHD syndrome and the BHD–MTOR (mammalian target of rapamycin) pathway, and could ultimately provide a useful preclinical model for molecular targeting by novel therapeutics.

Here we report the establishment and characterization of renal tumor cell line, UOK 257, by long-term tissue culture derived from a tissue sample from a 46-year-old man with a particularly aggressive BHD clinical manifestation. Standard G-banding analysis revealed a complex karyotype. To better resolve the rearranged chromosomes, we used two molecular cytogenetic technologies, spectral karyotyping (SKY) [12] and fluorescence in situ hybridization (FISH) with gene-specific probes. We also used ultrastructural studies via electron microscopy to characterize subcellular morphology of organelles from the tumor cell.

Specifically, we applied FISH with gene-specific probes to reveal the chromosomal abnormalities involving loss of heterozygosity for several loci on chromosome arm 17p, such as the *TP53* and *FLCN* genes [8]. It is our hope that the multilevel cytogenetic and ultrastructural characterization of the BHD tumor cell line provided herein will assist further studies on the molecular mechanism of BHD tumorigenesis, the mechanism of organ selective metastasis, the genotype–phenotype relationship, the identification of molecular markers for diagnosis or prognosis, and the discovery of novel therapeutic drugs for the BHD syndrome.

2. Materials and methods

2.1. Case report

The patient was a previously healthy 46-year-old man who initially presented with acute-onset gross hematuria. His past medical history was significant for history of two previous episodes of spontaneous pneumothorax and the diagnosis of numerous fibrofolliculomas on the scalp, face, neck, and trunk. During his workup for hematuria, computed tomographic (CT) scan of the chest, abdomen, and pelvis revealed a 7- by 5-cm multinodular enhancing mass encompassing the upper pole of the left kidney, no solid lesions in the right kidney, and multiple pulmonary cysts. Otherwise, CT scan revealed no evidence of disease in the remainder of the chest, abdomen, and retroperitoneum.

Given both the dermatologic findings and the renal mass, the patient underwent genetic testing and was found to have a germline mutation in the *FLCN* gene and a diagnosis of BHD syndrome was made. Following diagnosis and evaluation, the patient underwent an open left radical nephrectomy via an 11th-rib flank incision.

Pathologic examination revealed clear cell RCC, Fuhrman grade 3 of 4, with evidence of invasion into the hilar adipose tissue. Multiple hilar lymph nodes, removed at the time of resection, revealed no evidence of tumor. Furthermore, although the mass was predominantly clear cell RCC, the pathologist noted foci of tubular papillary and chromophobe histologic type.

Approximately eight months after surgery, the patient presented with a 4-day history of abdominal discomfort and diarrhea. A CT scan of the abdomen and pelvis revealed a 3-cm soft tissue mass in the left renal fossa. The patient subsequently underwent a percutaneous CT-guided biopsy of the retroperitoneal mass, which revealed recurrent RCC that was morphologically consistent with the patient's previous RCC tumor. Further imaging to identify metastases included a whole-body bone scan, magnetic resonance imaging of the head, and a whole-body PET scan. These revealed foci of metastatic disease in the left renal fossa, left iliac crest, and left lesser trochanter. He subsequently underwent several cycles of systemic therapy, including high-dose interleukin 2 (IL 2), interferon, and an investigational agent (phase I clinical trial). The disease continued to progress through the therapies, however, and the patient was eventually was placed on palliative care; ~21 months after initial diagnosis and 13 months after the diagnosis of metastatic disease, he died of progressive metastatic renal cancer.

2.2. Tumor origin and pathologic analysis

The surgical specimen from a left nephrectomy weighed 1,213.2 g and consisted of kidney and adrenal gland, with overlying fascia and adipose tissue. The tumor mass measured approximately 8.0 by 8.0 by 8.0 cm and had completely distorted the upper pole of kidney. The multiple nodules of friable tumor mass were present primarily in the superior pole of the kidney and were invading the collecting system. Further dissection revealed a yellow/tan homogeneous tumor mass within the nodule. A portion of the tumor was retained in the laboratory for viable in vitro culture, portions were submitted for electron microscopy, and the remainder was retained for permanent histopathologic diagnosis. Prior to surgery, the patient gave informed consent according to a tissue procurement protocol approved by the Institutional Review Board (IRB).

2.3. Tissue culture, establishment of transplantable cell line, and subclone lines

A portion of tissue was removed from the middle of the tumor mass ~10 minutes after nephrectomy and tissue extraction. Using sterile technique, the tissue was immersed into a small aliquot of 1× phosphate-buffered saline (PBS) buffer, minced with a sharp scalpel to obtain ~1-mm diameter fragments, and then plated onto a 60-mm Petri dish. Dulbecco's modified Eagle's medium (DMEM) containing high glucose (4.5 g/L), L-glutamine (2 mmol/L), supplemented with penicillin (50 units/mL), streptomycin (100 μg/mL), and MEM nonessential amino acids (1×, from 100× solution; Invitrogen Life Technologies,

Rockville, MD), with 10% of heat-inactivated fetal bovine serum, was slowly added to the Petri dish. The volume of medium was adjusted so that there was enough to cover the tissue fragments, but not enough to cause them to float. The culture was then incubated at 37°C in a humidified atmosphere containing 5% CO_2.

Approximately 36 hours after plating, adherent epithelial cell outgrowth from tissue debris was observed. An additional 1–2 mL of fresh DMEM was then added. The first passage was performed 3–5 days after plating, by a light treatment with 0.05% trypsin–EDTA while monitoring the cells under an inverted tissue culture microscope. Subsequent passages were performed every 3–5 days in the same manner. The line was propagated for over 50 passages. The established primary line was designated UOK 257.

From the parental stock of passage 6, limiting dilutions were performed, and resulting subclones were isolated and cultured for more than 15 passages. The subclones were numbered, following the name of the primary line; for example, UOK 257 SC6 refers to subclone 6 of the primary cell line UOK 257.

Approximately 3×10^6 cells in 0.2 mL 1× PBS was subcutaneously injected into SCID/BEIG mice to determine the tumorigenic potential of the cells. Xenograft tumor specimens were reimplanted into new mice for multiple generations, and xenografts from the mice were also cultured in the laboratory. Animal care protocols were approved by the Institutional Animal Care and Use Committee (IACUC) and were in accordance with the guidelines of the National Cancer Institute.

2.4. Cell proliferation and metaphase preparation

When the UOK 257 line culture reached the proliferation phase (i.e., seeded at ~40% confluence and grown and harvested on the third day at ~ 90% confluence), the proliferative activity and cellular kinetics were analyzed using an automated flow cytometer (BD FACScalibur E1806; BD Biosciences, San Jose, CA). The protocol and technical control used was as previously described [13] with some modifications. Briefly, the cells (10^6/mL) were washed with PBS and fixed in 70% ethanol for at least 1 hour, or the cells were incubated at 4° C overnight, washed twice with PBS, and incubated with 50 μL of RNase in 1 mL PBS plus 0.1% bovine serum albumin for 30 minutes.

A DNA histogram was obtained by staining cells with 7-aminoactinomycin D (7-AAD) at 5 μL (0.25 μg)/10^6 cells (BD Biosciences Pharmingen, San Jose, CA) and incubating 10 minutes before analysis. Data were analyzed by using FlowJo version 6.3.2 software (Tree Star, Ashland, OR).

At passage 18, UOK 257 cells were treated with colcemid (10 μL/mL, Boehringer Mannheim–Roche Diagnostics Corporation, Indianapolis, IN) for 1 hour, then subjected to hypotonic treatment (0.075 mol/L KCl) and fixative (methanol–acetic acid, 3:1) as previously described [12]. Chromosome spreads were prepared in a humidity chamber (Model CDS-5; Thermotron Industries, Holland, MI). Metaphase chromosome preparation was as previously described [14].

2.5. Cell pellet fixation and thin section for ultrastructural studies

Cell monolayers were washed with PBS, scraped, and fixed in 2.5% PBS-buffered glutaraldehyde, postfixed in osmium tetroxide, dehydrated, and embedded in Spurr's epoxy resin. Ultrathin sections were stained with uranyl acetate and lead citrate and were viewed in a transmission electron microscope (Model CM10; Philips Electronics, Mahwah, NJ).

2.6. DNA probe preparation and DNA sequencing analysis

Bacterial artificial chromosome–based DNA hybridization probes for FISH were prepared by using a Vysis nick-translation kit (Abbott Molecular–Vysis, Des Plaines, IL) incorporating SpectrumOrange or SpectrumGreen. SKY painting probes were prepared in-house, as detailed in: http://www.riedlab.nci.nih.gov/protocols.asp. Germline mutation sequencing analysis for the cell line was performed on an ABI PRISM 310 genetic analyzer (Perkin Elmer–Applera Applied Biosystems, Foster City, CA).

2.7. SKY analysis and FISH with chromosome-specific probes

Fifteen UOK 257 metaphase spreads were analyzed and scored for chromosome number (ploidy) and for numerical and structural aberrations. Spectrum-based classification and analysis of the fluorescent images was performed by using SkyView software (Applied Spectral Imaging [ASI], Vista, CA). The chromosome complements of every metaphase spread were analyzed and the karyotypes were described according to human chromosome nomenclature standards described in ISCN 2005 [15]. FISH analysis with a chromosome painting probe for chromosome 8 and a locus-specific gene probe for *MYC* (8q24.3) (Abbott Molecular–Vysis) was used to assess the copy number of this oncogene and to better define aberrant chromosomes containing small portions of chromosome 8.

Structural aberrations are considered clonal if two or more cells contain the same aberration [15]. With respect to numerical aberrations, gains of chromosomes are considered clonal if two or more cells contain the same extra chromosome, and losses are classified as clonal if they are observed in three or more cells [15].

The karyotype for UOK 257 (see figure in section 3.4, SKY analysis) has been entered into the NCBI SKY/CGH interactive online database (http://www.ncbi.nlm.nih.gov/sky/skyweb.cgi) with Padilla-Nash as submitter. Public access takes effect upon publication of the present article. In

this database, the patient's karyotypes are depicted as a colored human idiogram, called a SKYGRAM. Each SKYGRAM presents the complement of normal and abnormal chromosomes, with the position of their breakpoints linked to the NCBI DNA sequence database.

2.8. Image acquisition

The UOK 257 cell morphology was examined with an inverted microscope with a digital camera (1X71, Olympus Optical Co., Japan). Images were acquired with a 10× objective from 6–8 random fields per culture. The cell counting and mean cell size were analyzed with a Cellometer Auto T4 image-based cell counter (Nexcelom Bioscience, Lawrence, MA). The thin-section ultrastructural images were taken on a Zeiss EM109 electronic microscope (at ×6,500, ×11,000, and ×21,000 magnification). FISH fluorescence images were acquired with a Leica DMR XA fluorescent microscope (Leica Microsystems, Wetzlar, Germany) and analyzed by using IPLab version 3.7 image processing software (BD Biosciences Bioimaging, Rockville, MD) and customized scripts. Image acquisition of SKY-labeled metaphase chromosome spreads was performed by using a SpectraCube (Applied Spectral Imaging, Vista, CA) and a charge-coupled device camera on top of an epifluorescence microscope equipped with custom-designed-triple band pass optical SKY filter (Chroma Technology, Rockingham, VT). Analysis of the metaphase spreads for karyotyping was performed by using SkyView software (ASI, Vista, CA) [12].

3. Results

3.1. Histopathology

Figure 1 (A–D) shows the light microscope appearance of an aggressive RCC derived from this individual surgical

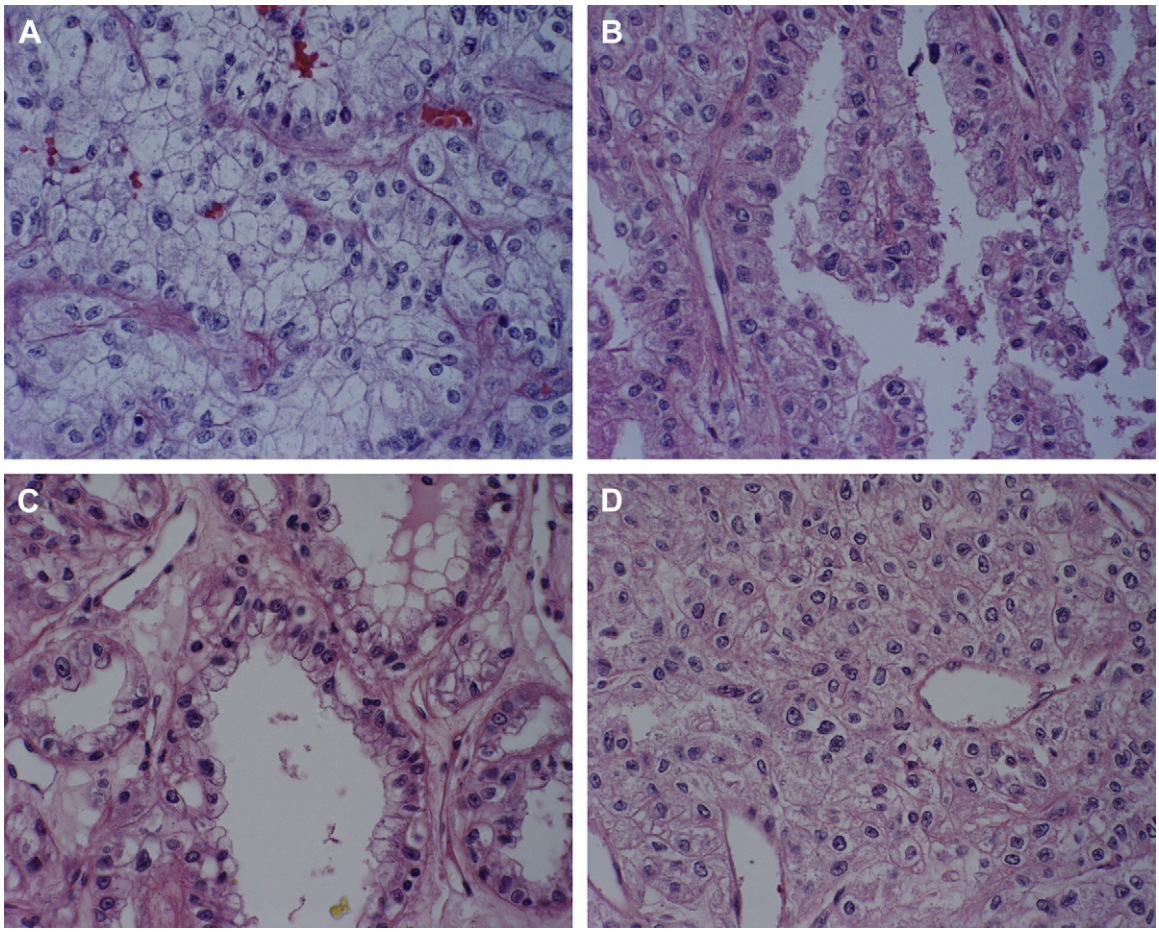

Fig. 1. Light microscopic appearance of different histologic types (A–D), kidney tumor mass samples from a patient with Birt–Hogg–Dubé (BHD) syndrome: (A) large areas composed of nests of clear cells with enlarged, round to irregular nuclei with prominent nucleoli and abundant vacuolated cytoplasm, scattered atypical naked nuclei (×400); (B) papillae lined by atypical epithelial cells with granular eosinophilic cytoplasm (×400); (C) atypical lining of the tubular structures (×400); and (D) histologically reminiscent foci of chromophobe renal cell carcinoma (×400). Tumor xenografts (E–H) revealed histologic features similar to those of the case pathologic report: (E) clear cell areas throughout the tumor (×400); (F) papillary architecture (×200); (G) areas with histologic resemblance to chromophobe (×200); and (H) solid areas of cells with eosinophilic cytoplasm, junction with complex of different histologic type (×200).

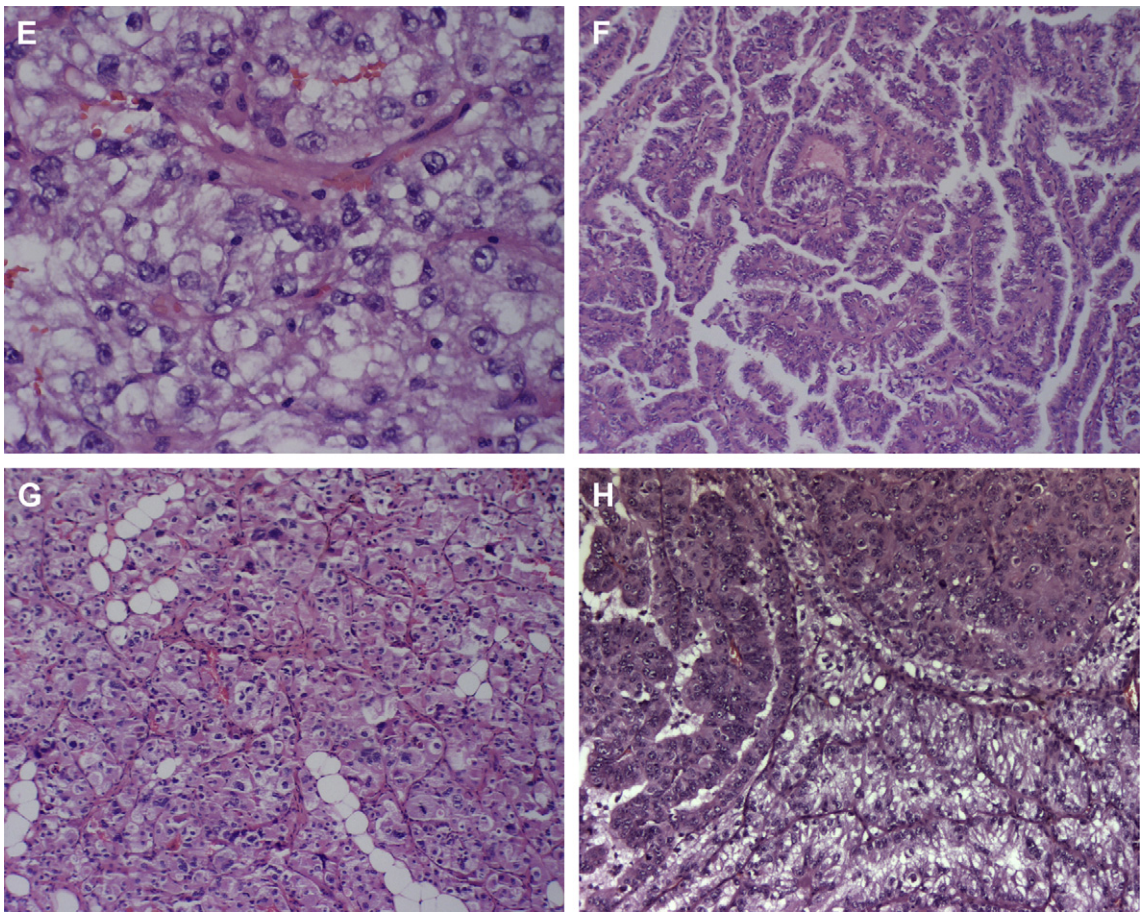

Fig. 1. (*Continued*)

specimen. The tumor was characterized as predominantly atypical clear epithelial cell type (Fig. 1A), with enlarged, round to irregular nuclei, prominent nucleoli, and moderate to abundant vacuolated cytoplasm seen as single cells, clusters, and sheets. The tumor also demonstrated a variety of histologic types with detailed junctional complexity, including tubular papillaries (Fig. 1B), solid areas (Fig. 1C), and, notably, foci reminiscent of chromophobe RCC (Fig. 1D).

Ten SCID/BEIG mice injected with the UOK 257 primary cell line showed outgrowth within 3 weeks after injection, and palpable tumors were formed in 10 out of 10 mice. At 22 weeks after injection, tumor size was 1.5 cm in diameter. Hematoxylin–eosin stained slides were processed from tumor xenografts, revealing pathologic features similar to those of the case report. Notably, in some of the slower growing tumors, aged 28 weeks in mice by the time of euthanization, pathologic analysis showed features not only of the predominantly clear cell type (Fig. 1E), but also complex junctions with papillary architecture, solid areas of cells with eosinophilic cytoplasm lined by clear cells (Fig. 1H), and chromophobe foci surrounding the clear cell tumor area (Fig. 1G).

Concurrently, xenograft tumor specimens were reimplanted into new mice for several generations. These were brought back to the laboratory for proliferation cultures, and retained the ability to grow in culture. A subline derived from the xenograft, designated UOK 257 XRP1, when injected back into SCID/BEIG mice, resulted in a more rapid outgrowth than the parent line.

3.2. Cell proliferation, cell cycle distribution, and ploidy pattern

Morphologic aspects of primary human hereditary renal carcinoma cultures are shown in Figures 2A and 2B. The UOK 257 cells cultured in vitro show an adherent monolayer cultured epithelial cell phenotype and display a loss of contact inhibition. Unlike other renal cell lines, the UOK 257 cells form into small patches of cellular islands in culture at ~50% confluence. Cell cycle and ploidy pattern of UOK 257 cells were evaluated by flow cytometric DNA histogram of tumor cells stained with 7-AAD, which were cultured for 3 days to reach ~90% confluence. The distribution of the tumor cell population at each phase in the cell cycle is given in Figure 2C.

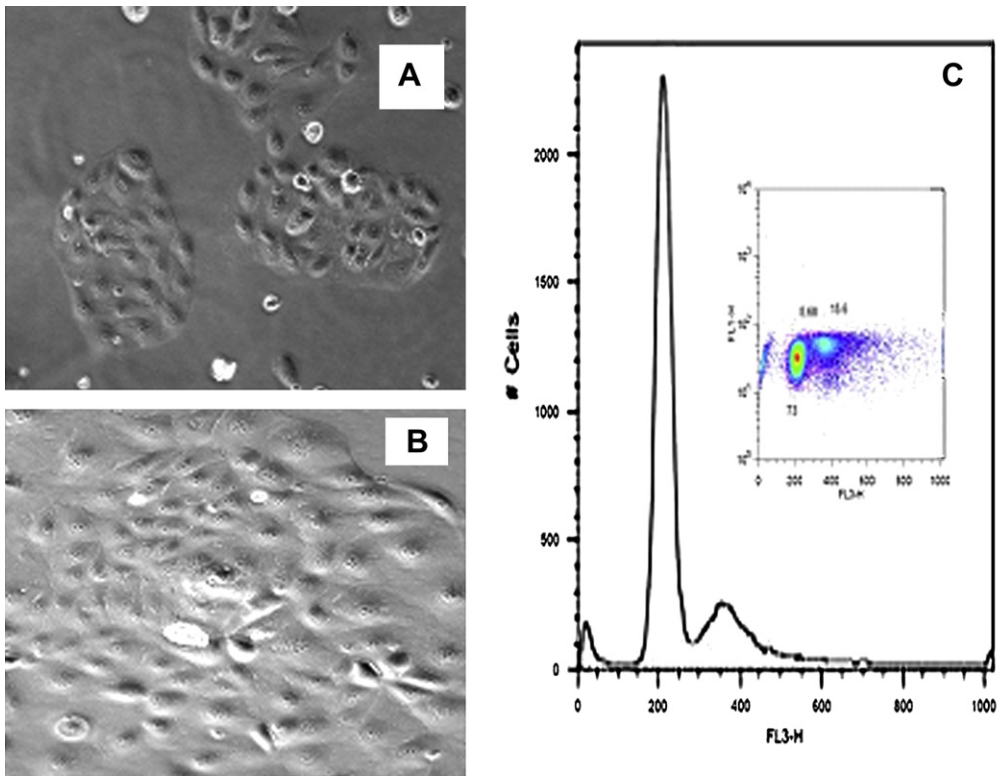

Fig. 2. Morphology of UOK 257 at 50% confluence exhibits small patched islands (A); at 90% confluence, loss of contact inhibition is evident (B). From flow cytometry, the scatterplot (C) and its one-dimensional histogram projection depict the cell cycle distribution of the tumor cell population.

3.3. Ultrastructural analysis

The cells exhibited ultrastructural features of tubular epithelial cells, such as microvilli on one (apical) surface and basal lamina on the opposite surface (Fig. 3A). Basal lamina-like material was focally abundant in between tumor cells (Fig. 3B). Desmosomes and tight junctions were present. Variable numbers of mitochondria were seen in the tumor cells. In some of them the mitochondria were abundant, consistent with oncocytic change (Fig. 3C). Cytoplasmic microvesicles similar to those present in chromophobe RCC were present in rare tumor cells (Fig. 3D). Some tumor cells contained a significant amount of glycogen, but lipid droplets were not common. The tumor cells were ultrastructurally comparable to those of the original tumor, which had also been examined ultrastructurally and which showed areas reminiscent of oncocytoma and chromophobe cell carcinoma.

3.4. SKY analysis

The composite SKY karyogram of UOK 257 at passage 18 is shown in Figure 4. The cell line is hypotriploid, with chromosome numbers ranging from 57 to 68 and a modal chromosome number of 65. The composite karyotype for UOK 257 was determined as 57~68<3n>,XX,−Y,+1,del(1)(p12)×2, del(3)(p12)×2,−4,+5,+6,der(6)t(6;17)(p11.2;q11.2)inv(6)(p25p11.2),der(6)t(6;17)(p11.2;q11.2)inv(6)(p25p11.2).ish t(6;8)(q27;q21)(MYC+),der(7)t(7;10)(q11.2;p12). ish +8 (MYC+),−9,+10,der(10)t(7;10)(q11.2;p11.2),der(10)t(1;7)(?;q32)t(7;10)(q11.2;p11.2),+12,−13,−14,+16,der(11;16)(p10;p10)[2],−18,−19,+20,−22[cp15].

SKY analysis reveals whole chromosome gains for 1, 5, 6, 8, 10, 12, 16, and 20 and whole chromosome losses for Y, 4, 9, 13, 14, 18, 19, and 22. SKY detected partial gains of 1q, 8q21~8qter (MYC+), and 10q and partial losses for 1p, and 3p. In addition, UOK 257 displayed an overall gain for 17q (four copies) and loss of 17p (two copies) due to the presence of two normal copies of chromosome 6 plus two unbalanced translocations, der(6)t(6;17) and der(6)t(6;8;17).

3.5. FISH with specific gene probes

Figure 5 depicts a metaphase spread analyzed by FISH with a probe for the *MYC* oncogene on chromosome 8. The copy number for *MYC* in UOK 257 is heterogeneous, with different metaphase spreads containing three, four, and up to five copies, including the unbalanced translocation der(6)t(6;8;17).

3.6. Sequencing analysis

We have confirmed the germline *FLCN* gene mutation from the primary UOK 257 cell line and in the single subcloned cell lines. The tumor lines showed the insertion of a C

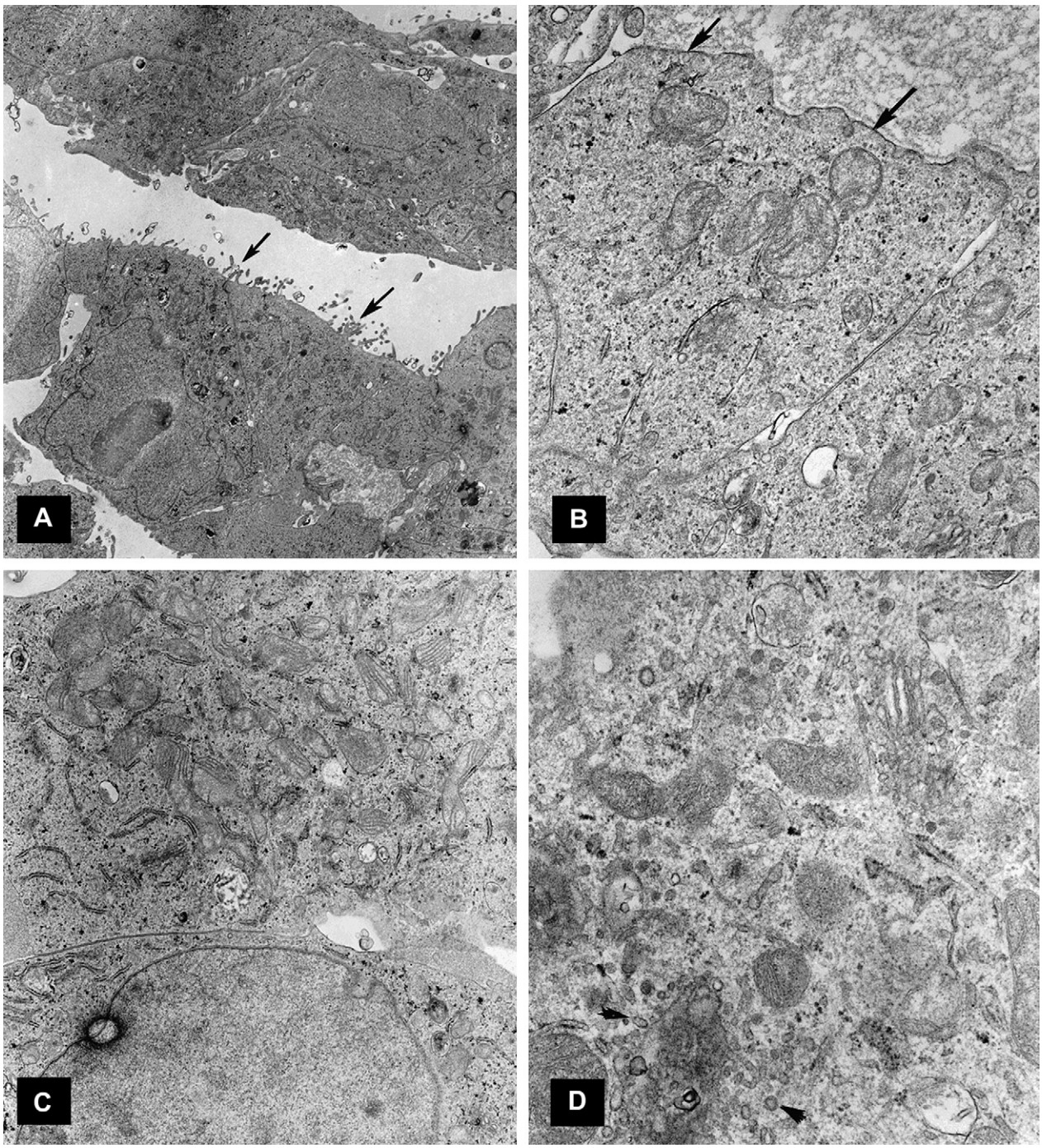

Fig. 3. (A–D) Ultrastructural features of findings from cultured UOK 257 tumor cells (90-nm thin section from fixed cell pellet) (×6,500). (A) Arrows indicate microvilli on one (apical) surface and basal lamina on the opposite surface. (B) Arrows indicate basal lamina-like material, focally abundant in between tumor cells. (C) Abundant mitochondria have appeared, consistent with oncocytic change. (D) Cytoplasmic microvesicles (arrowheads) were present in chromophobe renal cell carcinoma and rare tumor cells.

in nucleotide 1733, as shown in a sequencing chromatogram of DNA previously published [7]. This is the same mutation that had been found in the patient's germline. Notably, in the tumor lines, only the germline mutant copy is retained; the wild-type copy is lost (data not shown). Furthermore, the patient's germline mutation was present in the DNA from the implanted xenografts, confirming that the tumors were human in origin (data not shown).

Because the UOK 257 cell line was established from a predominantly clear cell type of tissue, we examined *VHL* gene mutation status. The wild-type *VHL* gene sequences were retained in this cell line.

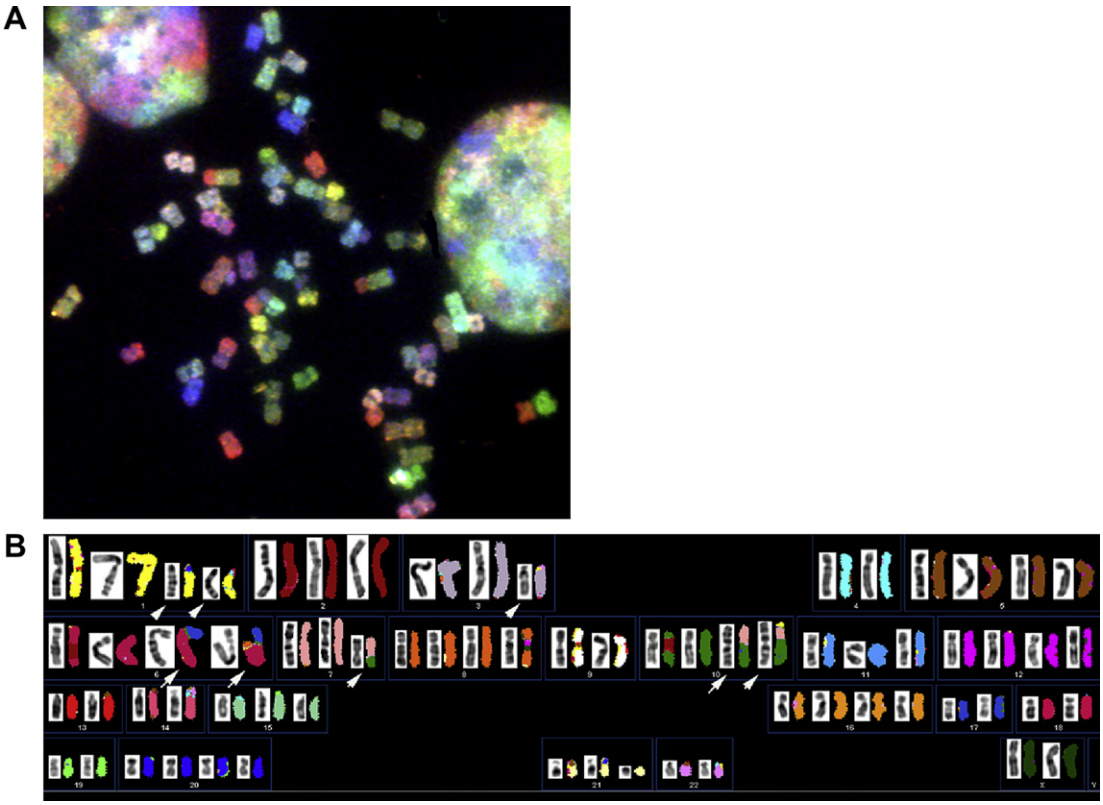

Fig. 4. (A) A representative metaphase spread from cell line UOK 257 at passage 18. (B). Composite karyotype of UOK 257 is near triploid, displaying multiple unbalanced translocations and deletions of chromosomes (white arrows). Inverted-DAPI stained chromosomes are at the left; pseudo-colored chromosomes to the right were hybridized with spectral karyotyping (SKY) probes.

4. Discussion

Here we report the establishment of a novel renal tumor cell line, UOK 257, derived from a patient with the hereditary cancer syndrome Birt–Hogg–Dubé. The cell line exhibits the same characteristics that are present in tumor cells representative of the BHD phenotype, and therefore provides a valuable resource for studying the mechanism of disease. In addition, UOK 257 is tumorigenic in SCID/BEIG mice, and thus allows for a xenograft model system in conjunction with an in vitro cell culture model.

Examination of the UOK 257 cell line reveals that it exhibits the same morphologic and ultrastructural features that are present in the tumor from which it was derived. Namely, the cells exhibit features of tubular epithelial cells, growing as an adherent monolayer and displaying loss of contact inhibition. Abundant mitochondria and cytoplasmic microvesicles are present, consistent with the features of the tumor. Notably, the histologic features of the original tumor are recapitulated in the tumors that arise in SCID/BEIG mice when UOK 257 is injected subcutaneously: predominantly clear cell tumors with areas of papillary architecture, eosinophilic cells, and chromophobic cells.

UOK 257 cells contain a mutant copy of the folliculin gene, *FLCN*, but have lost the wild-type copy, as revealed by DNA sequencing. The mutant copy contains an insertion of a C at nucleotide 1733 of *FLCN*, resulting in a frameshift mutation that is assumed to destroy the function of folliculin. This is a region that normally contains a tract of 8 Cs and is considered a hot spot for *FLCN* mutations, given that ~44% of known germline mutations consist of either an insertion or deletion of a C in this poly-C tract. Therefore, the UOK 257 cell line is useful for studying not only mutant *FLCN* function but also wild-type function in reconstituted lines.

The ploidy pattern of UOK 257 is consistent with patterns previously demonstrated for clear and papillary RCC, namely, predominantly diploidy with a certain percentage of aneuploidy [13,17]. UOK 257 is hypotriploid, with a modal chromosome number of 65. Notable chromosome losses include 3p, where the kidney cancer tumor suppressor gene *VHL* is located, and 17p, where *FLCN* is located, and there is a gain of chromosome 8, and an increase in copies of the *MYC* gene (between three and five copies), as determined by FISH. It is possible, therefore, that molecular pathways of *VHL*, *MYC*, and other genes may be contributing to the phenotype of this line, in addition to the loss of function of *FLCN*.

Due to the distinctive histologic, morphologic, and genomic characteristics of UOK 257 that correlate with tumor

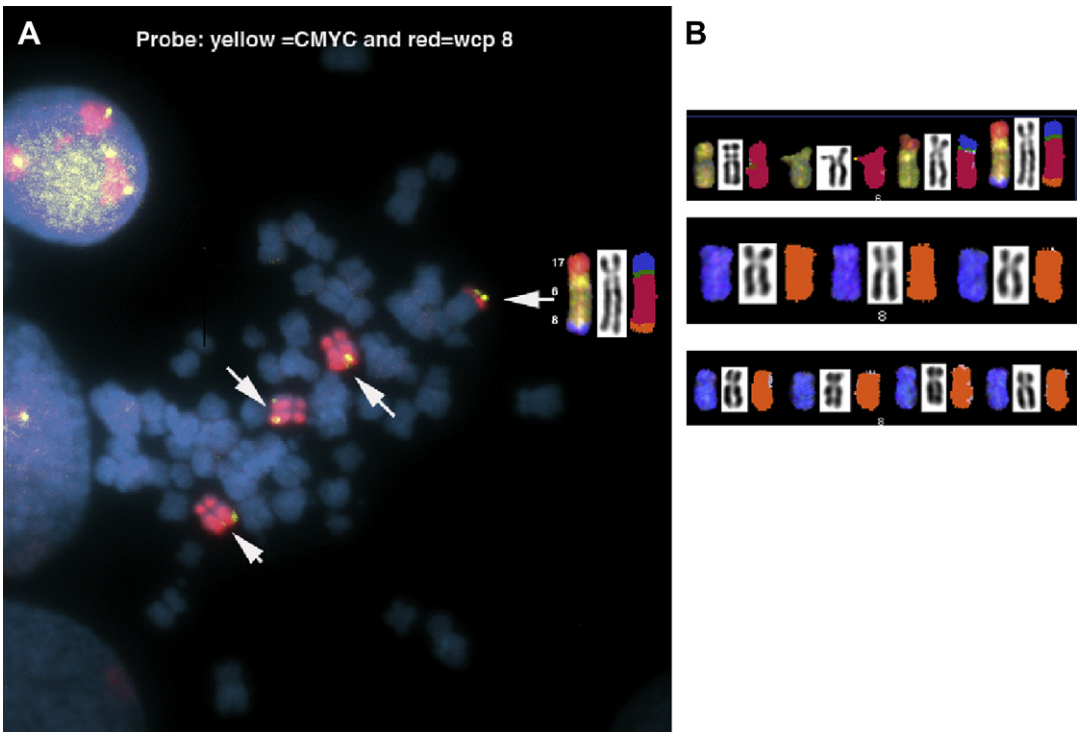

Fig. 5. Two clones of UOK 257 are revealed by SKY and FISH, one with three copies of chromosome 8 and the other with four copies of chromosome 8 found in 50% of cells. (A) Fluorescence in situ hybridization using a locus-specific probe for the *MYC* oncogene (yellow signal) and whole chromosome paint for chromosome 8 (red). (B) SKY analysis revealed further that 8q21~q24 (*MYC*) is fused to the distal region of the unbalanced translocation, der(6)t(6;17)t(6;8).

cells derived from Birt–Hogg–Dubé patients, as well as the potential to grow this line in vitro as well as in xenograft models, this cell line can serve as an extremely valuable resource in studying the mechanism of this disease. In addition, UOK 257 shares many characteristics with sporadic chromophobe renal carcinomas and renal oncocytomas and thus may serve as an excellent model to examine these diseases as well. Furthermore, this line can facilitate the ability to characterize molecular markers for diagnosis and prognosis of BHD, as well as potential drug therapies for the disease.

Acknowledgments

This research was supported in part by the Intramural Research Program of the U.S. National Institutes of Health, National Cancer Institute, Center for Cancer Research. The authors are grateful to Linda Stapleton-Barenboim for preparation of the SKY probes and to Jianping Huang and Zhiyu Li for assisting in flow cytometric facilities.

References

[1] Khoo SK, Bradley M, Wong FK, Hedblad MA, Nordenskjöld M, Teh BT. Birt–Hogg–Dubé syndrome: mapping of a novel hereditary neoplasia gene to chromosome 17p12-q11.2. Oncogene 2001;20:5239–42.

[2] Schmidt LS, Warren MB, Nickerson ML, Weirich G, Matrosova V, Toro JR, Turner ML, Duray P, Merino M, Hewitt S, Pavlovich CP, Glenn G, Greenberg CR, Linehan WM, Zbar B. Birt–Hogg–Dubé syndrome, a genodermatosis associated with spontaneous pneumothorax and kidney neoplasia, maps to chromosome 17p11.2. Am J Hum Genet 2001;69:876–82.

[3] Nickerson ML, Warren MB, Toro JR, Matrosova V, Glenn G, Turner ML, Duray P, Merino M, Choyke P, Pavlovich CP, Sharma N, Walther M, Munroe D, Hill R, Maher E, Greenberg C, Lerman MI, Linehan WM, Zbar B, Schmidt LS. Mutations in a novel gene lead to kidney tumors, lung wall defects, and benign tumors of the hair follicle in patients with the Birt–Hogg–Dubé syndrome. Cancer Cell 2002;2:157–64.

[4] Pavlovich CP, Walther MM, Eyler RA, Hewitt SM, Zbar B, Linehan WM, Merino MJ. Renal tumors in the Birt–Hogg–Dubé syndrome. Am J Surg Pathol 2002;26:1542–52.

[5] Tickoo SK, Reuter VE, Amin MB, Srigley JR, Epstein JI, Min KW. Renal oncocytosis: a morphologic study of fourteen cases. Am J Surg Pathol 1999;23:1094–101.

[6] Adley BP, Smith ND, Nayar R, Yang XJ. Birt–Hogg–Dubé syndrome: clinicopathologic findings and genetic alterations. Arch Pathol Lab Med 2006;130:1865–70.

[7] Vocke CD, Yang Y, Pavlovich CP, Schmidt LS, Nickerson ML, Torres-Cabala CA, Merino MJ, Walther MM, Zbar B, Linehan WM. High frequency of somatic frameshift *BHD* gene mutations in Birt–Hogg–Dubé-associated renal tumors [Erratum in: J Natl Cancer Inst. 2005;97:1096]. J Natl Cancer Inst 2005;97:931–5.

[8] Gad S, Lefèvre SH, Khoo SK, Giraud S, Vieillefond A, Vasiliu V, Ferlicot S, Molinié V, Denoux Y, Thiounn N, Chrétien Y, Méjean A, Zerbib M, Benoît G, Hervé JM, Allègre G, Bressac-de Paillerets B, Teh BT, Richard S. Mutations in *BHD* and *TP53* genes, but not in HNF1β gene, in a large series of sporadic chromophobe

renal cell carcinoma [Erratum in: Br J Cancer 2007;96:1314]. Br J Cancer 2007;96:336–40.

[9] Baba M, Hong SB, Sharma N, Warren MB, Nickerson ML, Iwamatsu A, Esposito D, Gillette WK, Hopkins RF 3rd, Hartley JL, Furihata M, Oishi S, Zhen W, Burke TR Jr, Linehan WM, Schmidt LS, Zbar B. Folliculin encoded by the *BHD* gene interacts with a binding protein, FNIP1, and AMPK, and is involved in AMPK and mTOR signaling. Proc Natl Acad Sci U S A 2006;103:15552–7.

[10] Garvin AJ, Re GG, Tarnowski BI, Hazen-Martin DJ, Sens DA. The G401 cell line, utilized for studies of chromosomal changes in Wilms' tumor, is derived from a rhabdoid tumor of the kidney. Am J Pathol 1993;142:375–80.

[11] Williams RD, Elliott AY, Stein N, Fraley EE. In vitro cultivation of human renal cell cancer: I. Establishment of cells in culture. In Vitro 1976;12:623–7.

[12] Schröck E, du Manoir S, Veldman T, Schoell B, Wienberg J, Ferguson-Smith MA, Ning Y, Ledbetter DH, Bar-Am I, Soenksen D, Garini Y, Ried T. Multicolor spectral karyotyping of human chromosomes. Science 1996;273:494–7.

[13] Li G, Cottier M, Sabido O, Gentil-Perret A, Lambert C, Genin C, Tostain J. Different DNA ploidy patterns for the differentiation of common subtypes of renal tumors. Cell Oncol 2005;27:51–6.

[14] Padilla-Nash HM, Barenboim-Stapleton L, Difilippantonio MJ, Ried T. Spectral karyotyping analysis of human and mouse chromosomes. Nat Protoc 2006;1:3129–42 [Available at: http://www.nature.com/nprot/journal/v1/n6/abs/nprot.2006.358.html].

[15] ISCN 2005: an international system for human cytogenetic nomenclature (2005). Shaffer LG, Tommerup N, editors. Basel: S. Karger, 2005.

[16] Kuroda N, Toi M, Hiroi M, Shuin T, Enzan H. Review of renal oncocytoma with focus on clinical and pathobiological aspects. Histol Histopathol 2003;18:935–42.